Frequency-domain Iterative Parallel Interference Cancellation for Multicode DS-CDMA-MIMO Multiplexing

Akinori Nakajima, Garg Deepshikha, and Fumiyuki Adachi
Dept. of Electrical and Communications Engineering, Graduated school of Engineering,
Tohoku University, Sendai, Japan
nakajima@mobile.ecei.tohoku.ac.jp

Abstract— **In a multicode DS-CDMA transmission, high-speed data rate can be achieved by using orthogonal code multiplexing while retaining the multi access capability. For further increase of the transmission data rate, the use of multi-input multi-output (MIMO) multiplexing is very effective. However, channels become severely frequency-selective, as a result, the performance is severely degraded in a frequency-selective fading channel due to orthogonality distortion among spreading codes. Recently, we proposed an iterative parallel interference cancellation (PIC) for SC-MIMO multiplexing in a frequency-selective fading channel. In this paper, we apply the frequency-domain iterative PIC to multicode DS-CDMA MIMO multiplexing in a frequency-selective fading channel and investigate, by the computer simulation, the impact of spreading factor and channel frequency-selectivity on the achievable bit error rate (BER) performance. Packet access will be the core technology of the next generation mobile communications systems. As an efficient error control technique, rate compatible punctured turbo coded hybrid automatic repeat request (RCPT-HARQ) is well known. We also evaluate, by computer simulation, the throughput performance of RCPT-HARQ in a frequency-selective Rayleigh fading channel.**

Keywords- Multicode DS-CDMA, MIMO multiplexing, iterative PIC, Turbo coded Hybrid ARQ, mobile communication

I. INTRODUCTION

Recently, there have been tremendous demands for high-speed data transmissions higher than few tens of Mbps in mobile communications [1]. However, for such high-speed data transmissions, the channel consists of many resolvable paths with different time delays, resulting in a severely frequency-selective fading channel. If multicode DS-CDMA is used, the transmission performance is severely degraded due to distortion of the orthogonality among orthogonal spreading codes. It has been shown that the use of frequency-domain equalization (FDE) can significantly improve the transmission performance of multicode DS-CDMA [2].

For wireless communication, the available bandwidth is limited, so much higher spectrum-efficient transmission technique is required for the next generation mobile communication systems. One of the promising techniques is the multiple-input multiple-output (MIMO) multiplexing [3] that uses multiple transmit and receive antennas. In MIMO multiplexing, a transmit data sequence is transformed into parallel sequences and each sequence is transmitted from a different transmit antenna at the same time with the same carrier frequency. Therefore, the total transmission data rate increases in proportion to the number of transmit antennas without requiring additional bandwidth. At a receiver, it is necessary to separate the signals transmitted from different antennas. A lot of research attention has been paid to find the signal separation methods which provide a performance close to that of maximum likelihood detection (MLD) but with reduced complexity, like vertical-Bell laboratories layered space-time architecture (V-BLAST) [4], MLD using QR decomposition [5] and so on. Recently, we proposed an iterative parallel interference cancellation (PIC) for SC-MIMO multiplexing in a frequency-selective fading channel [6]. In this paper, we apply the frequency-domain iterative PIC to multicode DS-CDMA-MIMO multiplexing. Packet access will be the core technology of the next generation mobile communication systems. Very high speed and high quality packet transmissions in a bandwidth-limited can be achieved by the joint use of MIMO multiplexing and hybrid automatic repeat request (HARQ). In this paper, we evaluate, by the computer simulation, the bit error rate (BER) performance of multicode DS-CDMA-MIMO multiplexing using frequency-domain iterative PIC and the throughput performance of HARQ combined with rate compatible punctured turbo (RCPT) code [7] in a frequency-selective Rayleigh fading channel.

The remainder of this paper is organized as follows. Section II describes the multicode DS-CDMA-MIMO multiplexing with the frequency-domain iterative PIC. Section III presents the computer simulation results of the BER performance and throughput performance in a frequency-selective Rayleigh fading channel. Section IV concludes the paper.

II. FREQUENCY-DOMAIN ITERATIVE PIC USING MULTICODE DS-CDMA-MIMO MULTIPLEXING

A. Transmitted and received signal

Fig.1 shows the transmitter and receiver structure of multicode DS-CDMA-(N_t,N_r)MIMO multiplexing using frequency-domain iterative PIC with N_t transmit antennas and N_r receive antennas. At the transmitter, turbo coding is performed on the CRC coded binary information sequence, and the transmitted sequences obtained by puncturing the turbo coded sequence are stored in the buffer. In this paper, RCPT type II HARQ S-P2 [8] is considered.

After bit-interleaving, data-modulation is applied to obtain a data symbol sequence $\{d(n')\ ;\ n'=0\sim CN_tN_c/SF-1\}$, where SF is the spreading factor, C is the code-multiplexing order and N_c is the block length in chips for fast Fourier transform (FFT). In this paper, QPSK data-modulation is considered. The QPSK symbol sequence is transformed into C parallel symbol sequences $\{d_c(n)\ ;\ n=0\sim N_tN_c/SF-1,\ c=0\sim C-1\}$ by serial/parallel (S/P) conversion and spreading operation is performed on each symbol sequence by using one of the SF orthogonal spreading codes. As a consequence, C parallel chip sequences are code-multiplexed into a single chip sequence. Scrambling is performed to make the transmitted orthogonal multicode DS-

0-7803-9152-7/05/$20.00 (c) 2005 IEEE

CDMA signal noise-like. The multicode DS-CDMA signal $s(t')$, $t' = 0 \sim N_t N_c - 1$, can be expressed as

$$s(t') = \left[\sum_{c=0}^{C-1} d_c(\lfloor t'/SF \rfloor) c_c(t')\right] c_{scr}(t') \text{ , (1)}$$

where $c_c(t')$ is the cth orthogonal code and $c_{scr}(t')$ is the scramble sequence.

For MIMO multiplexing, $s(t')$ is transformed by S/P-converter into N_t parallel chip sequences $\{s_{n_t}(t)$; t=0~N_c-1, n_t=0~N_t-1$\}$ to be transmitted from different transmit antennas. Each chip sequence has a length of N_c chips. The last N_g chips in the block is copied and inserted as a cyclic prefix into the guard interval (GI) placed at the beginning of each block. After GI insertion, N_t blocks are transmitted simultaneously from N_t transmit antennas using the same carrier frequency.

N_t transmitted blocks go through different frequency-selective fading channels. Each channel is assumed to be a chip-spaced L-path frequency-selective fading channel. At the receiver, a superposition of N_t transmitted signals is received by N_r antennas. After the removal of GI from the received signal, N_c-point FFT is applied to decompose the GI-removed received signal $r_{n_r}(t)$, t=0~N_c-1, into N_c frequency components. The kth frequency component $R_{n_r}(k)$ of the received signal on the n_rth antenna can be expressed as

$$R_{n_r}(k) = \sqrt{2S}\sum_{n_t=0}^{N_t-1} H_{n_r,n_t}(k) S_{n_t}(k) + \Pi_{n_r}(k) \text{ , (2)}$$

where S is the received signal power per antenna, $H_{n_r,n_t}(k)$ is, the complex channel gain between the n_tth transmit antenna and the n_rth receive antenna, $S_{n_t}(k)$ is the transmitted signal component, and $\Pi_{n_r}(k)$ is the noise component. They are given by

$$\begin{cases} H_{n_r,n_t}(k) = \sum_{l=0}^{L-1} h_{n_r,n_t,l} \exp(-j2\pi\tau_l k/N_c) \\ S_{n_t}(k) = \sum_{t=0}^{N_c-1} s_{n_t}(t) \exp(-j2\pi t k/N_c) \\ \Pi_{n_r}(k) = \sum_{t=0}^{N_c-1} n_{n_r}(t) \exp(-j2\pi t k/N_c) \end{cases} \text{ , (3)}$$

where $h_{n_r,n_t,l}$ denotes the lth path gain between the n_rth receive antenna and n_tth transmit antenna, $n_{n_r}(t)$ is a zero-mean complex Gaussian process having variance $2N_0/T_c$ with N_0 being the one-sided power spectrum density of additive white Gaussian noise (AWGN) and T_c is the chip length.

B. Frequency-domain iterative PIC

At first (i=0), two-dimensional (2D) FDE based on minimum mean square error (MMSE) criterion is used to suppress the inter-chip-interference (ICI) and the interference from signals transmitted from other antennas. However, 2D-MMSE-FDE can not suppress interference sufficiently. Hence, we perform one-dimensional (1D) MMSE-FDE and frequency-domain PIC in an iterative fashion. Fig.2 shows the frequency-domain iterative PIC. The kth frequency components after MMSE-FDE in the ith iteration are represented by N_t-by-1 vector $\widetilde{\mathbf{R}}^{(i)}(k) = [\widetilde{R}_0^{(i)}(k), \cdots, \widetilde{R}_{N_t-1}^{(i)}(k)]^T$.

1) 2D-MMSE-FDE (i=0)

The kth frequency component vector $\widetilde{\mathbf{R}}^{(0)}(k)$ after 2D-MMSE-FDE in the i=0th iteration can be expressed as

$$\widetilde{\mathbf{R}}^{(0)}(k) = \mathbf{W}^{(0)}(k)\mathbf{R}(k) \text{ , (4)}$$

where $\mathbf{R}(k) = [R_0(k), \cdots, R_{N_r-1}(k)]^T$ is the N_r-by-1 received signal vector at the kth frequency. $\mathbf{W}^{(0)}(k)$ is the N_t-by-N_r MMSE weight matrix and can be derived from [9] as

$$\mathbf{W}^{(0)}(k) = \mathbf{H}^H(k)[\mathbf{H}(k)\mathbf{H}^H(k) + (C \cdot E_c / N_0)^{-1}\mathbf{I}]^{-1} \text{ , (5)}$$

where $\mathbf{H}(k)$ is the N_r-by-N_t complex channel gain matrix whose

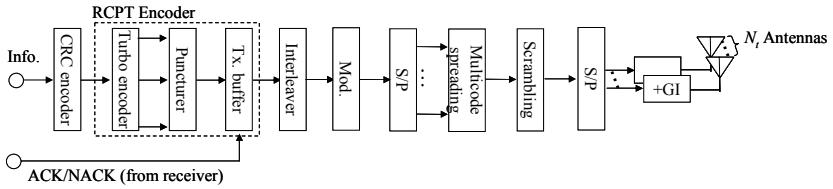

(a) Transmitter

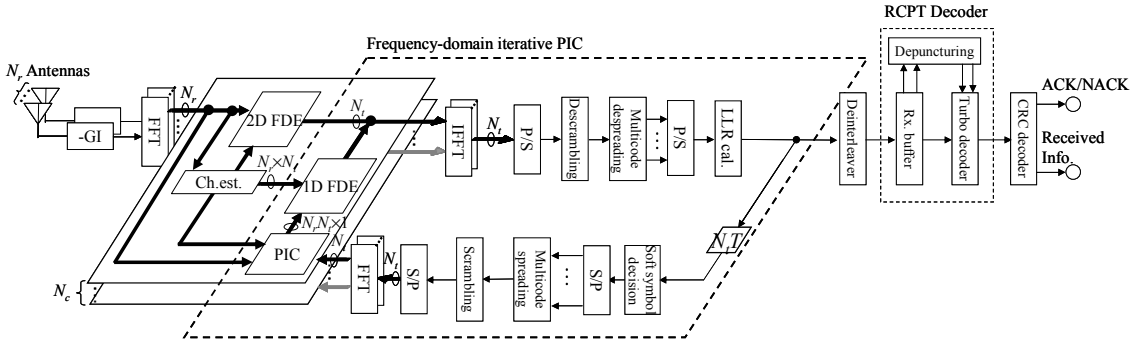

(b) Receiver

Figure 1 Transmitter and receiver structure.

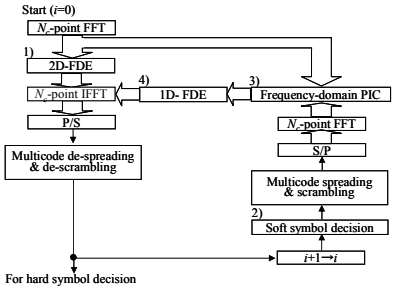

Figure 2 Frequency-domain iterative PIC.

component of the n_tth column and n_tth row is $H_{n_r,n_t}(k)$, E_c/N_0 ($=ST_c/N_0$) represents the average received chip energy per code-to-AWGN power spectrum density ratio, **I** is the N_r-by-N_r identity matrix, and $(.)^H$ is the Hermit transpose operation.

2) Soft symbol replica generation

The multicode signal $\tilde{s}_{n_t}^{(i)}(t)$, t=0~N_c-1, in the time-domain is obtained by performing N_c-point IFFT on $\{\tilde{R}_{n_t}^{(i)}(k)$; k=0~N_c-1$\}$ after carrying out the ith MMSE-FDE. N_t parallel blocks $\{\tilde{s}_{n_t}^{(i)}(t)$; n_t=0~N_t-1$\}$ are transformed by P/S converter into the multicode signal $\tilde{s}^{(i)}(t')$. After descrambling and multicode despreading, the decision variable $\tilde{d}_c^{(i)}(n)$ of the nth symbol of the cth parallel symbol sequence sequence, c=0~C~1, is obtained as

$$\tilde{d}_c^{(i)}(n) = (1/SF)\sum_{t'=nSF}^{(n+1)SF} \tilde{s}^{(i)}(t') c_c^*(t' \bmod SF) c_{scr}^*(t') \quad (6)$$

where * is the complex conjugate operation. Then, decision variables of C parallel symbol sequences are P/S-converted into $\{\tilde{d}_c^{(i)}(n')$; n' =0~CN_tN_c/SF-1$\}$, which is the decision variable associated with the transmitted QPSK symbol sequence $d(n')$.

For soft symbol decision, the log likelihood ratio (LLR), $LLR_b^{(i)}(n')$, of the bth bit in the n' th symbol is computed. Then, the soft QPSK symbol replica $\hat{d}^{(i+1)}(n')$ to be used in the (i+1)th iteration is generated using $\{LLR_b^{(i)}(n')$; b=0,1$\}$ [6]

$$\hat{d}^{(i+1)}(n') = \frac{1}{\sqrt{2}}\left\{\tanh(\beta\frac{LLR_0^{(i)}(n')}{2}) + j\tanh(\beta\frac{LLR_1^{(i)}(n')}{2})\right\}, \quad (7)$$

where β is a parameter that controls the extent to which the soft decision contributes to the replica generation. After performing multicode spreading and scrambling operations, the replicas of N_t parallel transmitted chip blocks, $\{\hat{s}_{n_t}^{(i+1)}(t)$; t=0~N_c-1, n_t=0~N_t-1$\}$, are obtained.

3) PIC operation

N_c-point FFT is performed on $\{\hat{s}_{n_t}^{(i+1)}(t)$; n_t=0~N_t-1$\}$ to obtain the frequency-domain signal replica $\{\hat{S}_{n_t}^{(i+1)}(k)$; k=0~N_c-1$\}$. For PIC operation, the frequency-domain interference replica $\sqrt{2S}\sum_{\substack{n_t'=0 \\ \neq n_t}}^{N_t-1} H_{n_r,n_t'}(k)\hat{S}_{n_t'}^{(i+1)}(k)$ is generated. Then, these replicas are subtracted from the signal component $R_{n_r}(k)$ received on the n_rth antenna to extract the signal component $\hat{R}_{n_r,n_t}^{(i+1)}(k)$ transmitted from the n_tth antenna. The PIC operation to extract $\hat{R}_{n_r,n_t}^{(i+1)}(k)$ is expressed as

$$\hat{R}_{n_r,n_t}^{(i+1)}(k) = R_{n_r}(k) - \sqrt{2S}\sum_{\substack{n_t'=0 \\ \neq n_t}}^{N_t-1} H_{n_r,n_t'}(k)\hat{S}_{n_t'}^{(i+1)}(k). \quad (8)$$

4) 1D-FDE (i>0)

Since ICI is partially eliminated from the received signals by performing PIC, the resulting signals are close to the case of single antenna transmission. Hence, when i>0, 1D-MMSE-FDE is used. Joint 1D-MMSE-FDE and N_r-branch antenna diversity combining is performed to obtain the signal component $\tilde{R}_{n_t}^{(i+1)}(k)$ at the kth frequency as

$$\tilde{R}_{n_t}^{(i+1)}(k) = \mathbf{W}_{n_t}^{(i+1)}(k)\hat{\mathbf{R}}_{n_t}^{(i+1)}(k), \quad (9)$$

where $\hat{\mathbf{R}}_{n_t}^{(i+1)}(k) = [\hat{R}_{0,n_t}^{(i+1)}(k), \cdots, \hat{R}_{N_r-1,n_t}^{(i+1)}(k)]^T$ represents the received kth frequency component of the signal vector transmitted from the n_tth antenna. $\mathbf{W}_{n_t}^{(i+1)}(k)$ is the 1-by-N_r equalization weight vector based on MMSE criterion for the (i+1)th iteration and is given by

$$\mathbf{W}_{n_t}^{(i+1)}(k) = \mathbf{H}_{n_t}^H(k)[\mathbf{H}_{n_t}^H(k)\mathbf{H}_{n_t}(k) + (C \cdot E_c/N_0)^{-1}]^{-1}, \quad (10)$$

where $\mathbf{H}_{n_t}(k)$ is the n_tth row vector of **H**(k).

The above processes 1)~4) are repeated a sufficient number of times. Then, data-demodulation is performed, followed by deinterleaving and RCPT decoding. In the RCPT decoder, depuncturing, turbo decoding, and error detection are performed. The result of error detection is transmitted to the transmitter as ACK/NACK.

III. RCPT TYPE II HARQ S-P2

In this paper, we consider RCPT type II HARQ S-P2 [8]. Fig.3 shows transmitted packet generation. In this paper, turbo encoder of coding rate R=1/3 is applied. The turbo encoder outputs the systematic bit (information bit) sequence and two parity bit sequences, each has length of K bits. The 1st transmit packet consists of the systematic bit sequence only and the 2nd and 3rd are taken from two punctured parity bit sequences. Puncturing matrices for the 1st, 2nd and 3rd transmissions are given by [8]

$$\begin{bmatrix}1 & 1\\ 0 & 0\\ 0 & 0\end{bmatrix}, \begin{bmatrix}0 & 0\\ 1 & 0\\ 0 & 1\end{bmatrix}, \begin{bmatrix}0 & 0\\ 0 & 1\\ 1 & 0\end{bmatrix}. \quad (11)$$

Fig.4 shows HARQ protocols. At the transmitter, the first packet consisting of systematic bit sequence only is transmitted. At the receiver, error detection is performed. If any error is detected in the received packet, an NACK is transmitted to the transmitter. Then, the second packet is

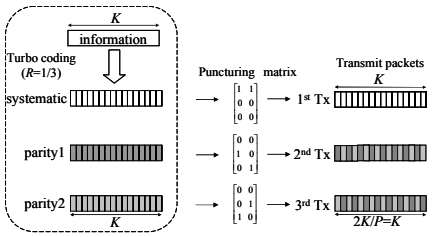

Figure 3 Transmit packet generation for RCPT type II HARQ S-P2.

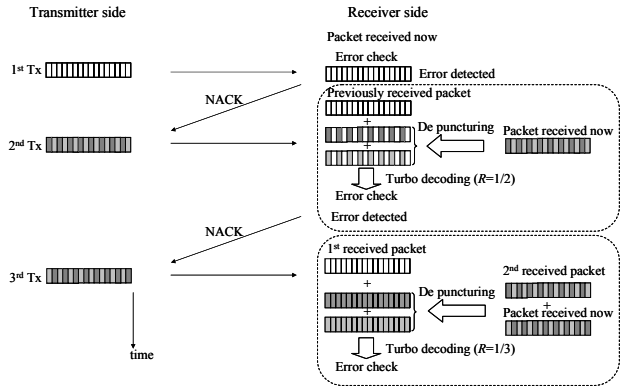

Figure 4 HARQ protocol.

transmitted. At the receiver, depuncturing is performed, followed by turbo decoding. The parity bits which have not been received yet are replaced by a channel value 0. In this case, turbo coding corresponds to R=1/2. After turbo decoding, the error detection is performed. If any error is detected, the receiver transmits the NACK again. At the transmitter, another punctured parity bit sequence is transmitted. In the receiver side, the second and third received packets are transformed into the two parity bit sequences by depuncturing and then, R=1/3 turbo decoding is carried out again.

IV. COMPUTER SIMULATION

The simulation parameters are given in Table 1. We assume an information bit sequence of K=2048 bits. Coding rate R=1/3 turbo encoder consisting of two (7,5) recursive systematic convolutional (RSC) encoders [10] is employed. We assume that N_r-by-N_t channels are independent and identically distributed frequency-selective block Rayleigh fading channels and have symbol-spaced exponentially decaying L=16-path power delay profile with decay factor α. Ideal channel estimation is assumed. Transmit chip block is a length of N_c=256 chips and the GI length of N_g=32 chips.

Fig. 5 plots the average BER performance of multicode DS-CDMA-(2,2)MIMO multiplexing as a function of the average received signal energy per bit-to-noise power spectrum density ratio E_b/N_0 per receive antenna when the equivalent spreading factor SF_{eq}(=SF/C) of 1 (i.e., the transmission data rate is the same as the chip rate for all SF) and SF=256. As the number of iterations increases, the BER performance improves and approaches that with perfect PIC. Perfect PIC provides the BER performance of (1,2)SIMO since interference from different antennas is cancelled perfectly. The use of 4 iterations is sufficient since the use of more than 4 iterations gives a negligible performance improvement. When α=0 and 6dB, E_b/N_0 degradation from perfect PIC for an average BER=10^{-4} reduces to about 0.1dB at the i=4th iteration.

Table 1. Simulation conditions.

Data Modulation		QPSK
Number of Tx, Rx antennas		N_t=N_r=2,4
Multicode spreading	Spreading modulation	BPSK
	Spreading factor	SF=1~256
Scramble code	M-sequence with a period of 4095 chips	
Channel	L=16-path black Rayleigh with exponential power delay profile	
	Decay factor α=0,6dB	

Fig. 6 plots the BER performance of multicode DS-CDMA-(2,2)MIMO multiplexing with SF as a parameter for SF_{eq}=1. The BER performance of SF=1 is almost the same as that of SF=256 when N_t=N_r=2 and α=0dB. However, when α=6dB, the performance dependency on SF is stronger than when α=0dB and the performance is better for larger SF. E_b/N_0 degradation for the average BER=10^{-4} from the perfect PIC is about 3.4, 0.8, and 0.1dB when SF=1, 16 and 256, respectively.

MMSE-FDE takes advantage of the frequency-selectivity of the channel and achieves a higher frequency diversity gain. Hence, MMSE-FDE provides better performance as the channel frequency-selectivity gets stronger. Although sufficient frequency diversity gain can not be obtained in a weak frequency-selective fading environment (i.e., α=6dB), the interference suppression is sufficient when SF is relatively large. As a consequence, multicode transmission with larger SF performance is less sensitive to the channel frequency-selectivity and closer to the perfect PIC.

Fig. 7 plots the throughput performance of RCPT type II HARQ S-P2 for multicode DS-CDMA-(N_t,N_r)MIMO multiplexing with i=4 as a function of the average received signal energy per symbol-to-noise power spectrum density ratio E_s/N_0 per receive antenna with SF as a parameter for the SF_{eq}=1. It can be seen from Fig. 7 that when α=0dB, the trend of throughput performance is the same as that of BER performance and close to the case of perfect PIC irrespective of SF. On the contrary, when α=6dB, the throughput depends on SF and as SF becomes larger, the performance becomes closer to perfect PIC. The throughput performance of SF=256(16) is, at most, about 1.2(1.1) and 1.4(1.3) times as good as that of SF=1 when (N_t,N_r)=(2,2) and (4,4), respectively. The throughput difference between SF=16 and 256 is larger when (N_t,N_r)=(4,4) than when (N_t,N_r)=(2,2), since the residual interference increases with the increase in the number of transmit antennas.

For comparison, the throughput performances of SIMO are also plotted in Fig. 7. When α=0dB, (2,2)MIMO multiplexing is about 2 times as good as (1,2)SIMO irrespective of SF; (4,4)MIMO multiplexing is about 3.5~4.0 times as good as (1,4)SIMO. On the other hand, when α=6dB, (2,2)MIMO multiplexing is about 1.7~2.0 times as good as (1,2)SIMO irrespective of SF and (4,4)MIMO multiplexing is about 2.7～4.0, 3.1~4.0 and 3.4～4.0 times as good as (1,4)SIMO for SF=1, 16 and 256, respectively.

V. CONCLUSIONS

In this paper, we applied a frequency-domain iterative PIC scheme to multicode DS-CDMA-MIMO multiplexing. We

evaluated, by computer simulation, the BER performance and the throughput performance of RCPT-HARQ in a frequency-selectivity Rayleigh fading channel and discussed the impacts of the channel frequency-selectivity and the spreading factor. It was shown that the use of 4 iterations is enough for performance improvement. For larger *SF*, the performance degradation from the perfect PIC is smaller irrespective of the channel frequency-selectivity. For the strong channel frequency-selectivity case (α=0dB), the throughput performance is insensitive to *SF*. On the other hand, for the weak frequency-selectivity case (α=6dB), the throughput performance is sensitive to *SF*; the throughput of *SF*=256 is, at most, 1.2and 1.4 times as good as that of *SF*=1.

REFERENCES

[1] F. Adachi, "Wireless past and future-evolving mobile communications systems," IEICE Trans. Fundamentals, vol.E84-A, pp.55-60, Jan. 2001.

[2] T. Itagaki, et al., "Joint frequency-domain equalization and antenna diversity combining for orthogonal multicode DS-CDMA signal transmissions in a frequency-selective fading channel," IEICE Trans. Commun., Vol. E87-B, No. 7, pp.1954-1963, July 2004.

[3] G. J. Foschini, et al., "On limits of wireless communications in a fading environment when using multiple antennas," Wireless Personal Commun., vol.6, no. 3, pp. 311-335, 1998.

[4] P. W. Wolniansky, et al., "V-BLAST: an architecture for realizing very high data rates over the rich-scattering wireless channel," Proc. ISSSE, pp.295-300, 1998.

[5] H. Kawai, et al., "Likelihood function for QRM-MLD suitable for soft-decision turbo decoding and its performance for OFCDM MIMO multiplexing in multipath fading channel," IEICE Trans. Commun., vol E88-B, No.1, pp.47-57, Jan. 2005.

[6] A. Nakajima, D. Garg, F. Adachi, "Throughput of turbo coded hybrid ARQ using single-carrier MIMO multiplexing," Proc. IEEE VTC2005-Spring, April 2005.

[7] D. N. Rowitch and L. B. Milstein, "Rate compatible punctured turbo (RCPT) codes in hybrid FEC/ARQ system," Proc. Comm. Theory Mini-conference of GLOBECOM'97, pp. 55-59, Nov. 1997.

[8] D. Garg and F. Adachi, "Rate compatible punctured turbo-coded hybrid ARQ for OFDM in a frequency selective fading channel," Proc. IEEE VTC2003-Spring, pp.2725-2729, Jeju, Korea, April 2003.

[9] John G. Proakis, *Digital Communications*, 4th edition, McGraw-Hill, 2001.

[10] J. P. Woodard and L. Hanzo, "Comparative study of turbo decoding techniques: an overview," IEEE Trans. Veh. Technol., vol.49, no.6, pp. 2208-2233, Nov. 2000.

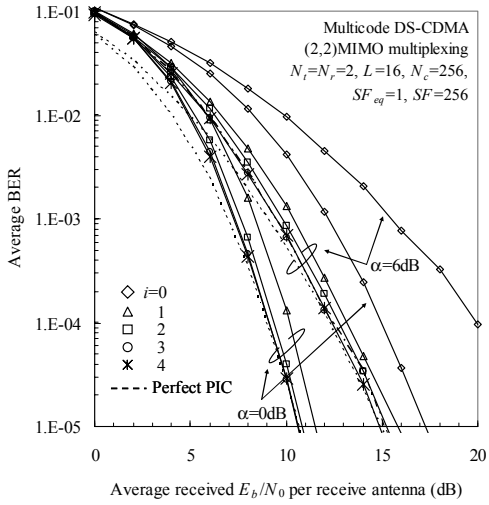

Figure 5 Effect of frequency-domain iterative PIC (*SF*=256).

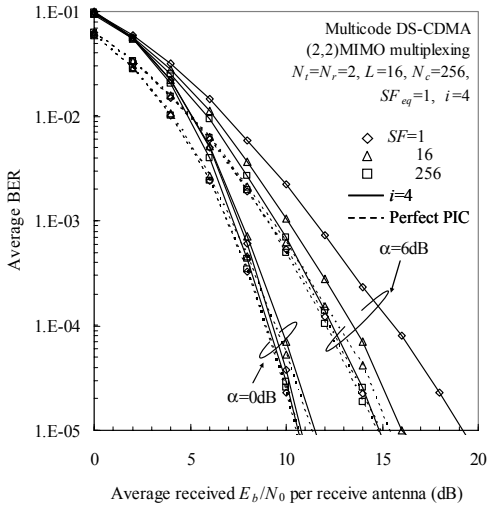

Figure 6 Effect of spreading factor (*i*=4).

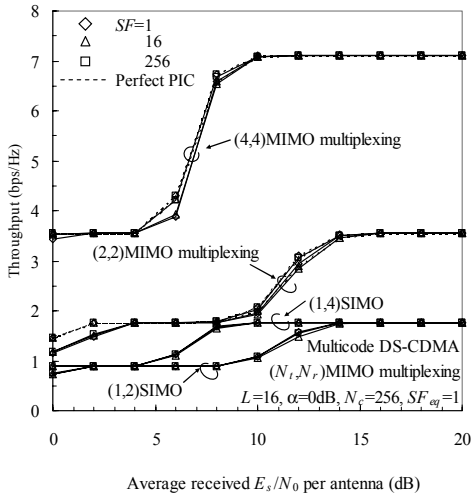

(a) α=0dB

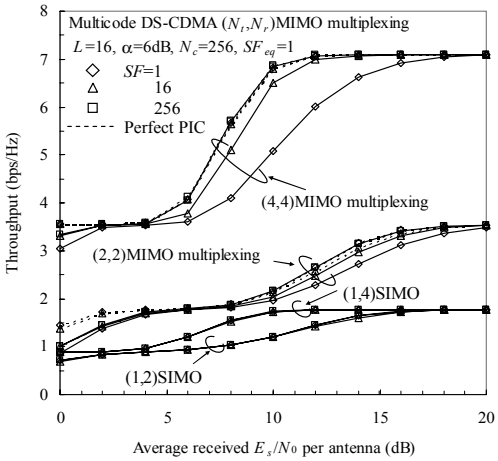

(b) α=6dB

Figure 7 Throughput performance of HARQ typeII S-P2.